Computer Methods and Programs in Biomedicine 140 (2017) 61–68

Contents lists available at ScienceDirect

Computer Methods and Programs in Biomedicine

journal homepage: www.elsevier.com/locate/cmpb

A methodology for automated CPA extraction using liver biopsy image analysis and machine learning techniques

Markos G. Tsipouras[a,b], Nikolaos Giannakeas[a,b], Alexandros T. Tzallas[a,b,*], Zoe E. Tsianou[a], Pinelopi Manousou[c], Andrew Hall[d], Ioannis Tsoulos[b], Epameinondas Tsianos[a]

[a] Division of Gastroenterology, Faculty of Medicine, School of Health Sciences, University of Ioannina, GR45110 Ioannina, Greece
[b] Department of Computer Engineering, School of Applied Technology, Technological Educational Institute of Epirus, Kostakioi, GR47100, Arta, Greece
[c] Liver Unit, St Mary's Hospital, Imperial College NHS Trust, London, UK
[d] Department of Histopathology, UCL Medical School, Royal Free Campus, Rowland Hill Street, London NW3 2QG, UK

ARTICLE INFO

Article history:
Received 6 February 2016
Revised 12 November 2016
Accepted 22 November 2016

Keywords:
Collagen proportional area
Liver biopsy image analysis
Machine learning techniques
Clustering
Classification

ABSTRACT

Background and objective: Collagen proportional area (CPA) extraction in liver biopsy images provides the degree of fibrosis expansion in liver tissue, which is the most characteristic histological alteration in hepatitis C virus (HCV). Assessment of the fibrotic tissue is currently based on semiquantitative staging scores such as Ishak and Metavir. Since its introduction as a fibrotic tissue assessment technique, CPA calculation based on image analysis techniques has proven to be more accurate than semiquantitative scores. However, CPA has yet to reach everyday clinical practice, since the lack of standardized and robust methods for computerized image analysis for CPA assessment have proven to be a major limitation.

Methods: The current work introduces a three-stage fully automated methodology for CPA extraction based on machine learning techniques. Specifically, clustering algorithms have been employed for background-tissue separation, as well as for fibrosis detection in liver tissue regions, in the first and the third stage of the methodology, respectively. Due to the existence of several types of tissue regions in the image (such as blood clots, muscle tissue, structural collagen, etc.), classification algorithms have been employed to identify liver tissue regions and exclude all other non-liver tissue regions from CPA computation.

Results: For the evaluation of the methodology, 79 liver biopsy images have been employed, obtaining 1.31% mean absolute CPA error, with 0.923 concordance correlation coefficient.

Conclusions: The proposed methodology is designed to (i) avoid manual threshold-based and region selection processes, widely used in similar approaches presented in the literature, and (ii) minimize CPA calculation time.

1. Introduction

Hepatitis C is one of the most common liver diseases worldwide, with 2%–3% of the world's population living with HCV infection [1]. Patients with chronic hepatitis C and elevated transaminases, which are candidates for treatment, often undergo liver biopsy for determination of hepatic fibrosis, i.e. determination of the collagen, which is the major component of fibrotic tissue. For assessing disease staging and provide diagnosis needle biopsy specimens are cut and stained using several dyes that bind selectively to liver collagen, making the quantification of the fibrosis suitable [2]. The most common dyes are the Masson's Trichrome for standard histological evaluation and the Sirius red for fibrosis detection. Pathologists assess the severity of HCV via microscopy images of liver biopsy specimens.

The liver biopsy evaluation systems, which are actually semiqualitative scores, are based on the assessment of architectural and structural findings in liver tissue. They assume that fibrosis generates around portals tracks and bridged from each portal track to other neighboring portals tracks, leading to the segmentation of liver tissue into dysfunctional areas. In this way, a staging of the disease is provided without taking under consideration the amount or degree of fibrosis. There are four scoring systems for the staging of liver diseases: a) the Knodell Histology Activity Index (HAI) [3], b) the Scheuer HAI [4], c) the Metavir scoring system [5], and d) finally the Ishak HAI [6]. Instead of the above approach, Manousou

* Corresponding author.
E-mail addresses: tsipouras@teiep.gr (M.G. Tsipouras), giannakeas@teiep.gr (N. Giannakeas), tzallas@teiep.gr (A.T. Tzallas), z.tsianou@gmail.com (Z.E. Tsianou), pinelopi.manousou@imperial.nhs.uk (P. Manousou), andrewhall1@nhs.net (A. Hall), itsoulos@teiep.gr (I. Tsoulos), etsianos@uoi.gr (E. Tsianos).

http://dx.doi.org/10.1016/j.cmpb.2016.11.012
0169-2607/

et al. [7], have indicated that CPA computation could provide also an effective way for liver disease staging estimation. The ratio of collagen in whole liver tissue (Collagen Proportionate Area – CPA), which can be measured in images, can quantitate the fibrosis, and has already been associated with the clinical course and outcome in patients with hepatitis C. Image analysis of liver biopsy images for CPA assessment has gained attention is the last decade, and has been used as a marker for fibrosis quantification in several studies.

In the extracted biopsy image, a number of needle tissue specimens are presented. According to the ideal assumption, only liver tissue should be placed on the substrate, as well as only fibrotic tissue should bind the dyes. Unfortunately, actual liver biopsy samples and the respective obtained images include several types of regions (beside liver tissue), with some of them retaining high dye concentrations. These can include: capsule or structural collagen, blood clots, blood vessels, muscles, fat, as long as artifacts such as dye drops, dust and scratches. The existence of all above undesired regions in the image makes the employment of sophisticated image analysis techniques imperative.

Although several works have been presented in the literature employing CPA assessment through image analysis, most of them mainly focus on the medical problem and attempt to correlate CPA with known HAI scores. Thus, include little details regarding the image analysis techniques [2,7–11]. Commonly, CPA analysis methodologies include a segmentation procedure (such as histogram thresholding) for detecting tissue and collagen areas and an additional artifact exclusion procedure, for the rejection of areas that should not be included in CPA calculation. Several research groups utilize image processing software, such as Zeiss KS300 [12], Adobe Photoshop [13], Nexus cube [14], or software that is provided with the microscope facility such as Aperio Image scope [8,9,11]. Some other authors clearly state that their methods are semi-automated, and thus extensive human interaction is needed. Such a method has been presented by Pillete et al. [15], where the image is converted into binary and then undesired areas are eliminated applying a semi-automated technique. Fibroquant, which is introduced by Masseroli et al. [16] employs histogram equalization, and several thresholding techniques [17,18]. This methodology has been also used by Caballero et al. [19]. A recent development for automated liver biopsy image analysis has been presented by Xu et al. [20]. In this study, a new index, namely qFibrosis, is introduced, which is based on extensive image processing, analyzing three area types (portal, fibrous and septa) in the image, and subsequently extracting several features from each of them, which are used for fibrosis staging. Thus, this work attempts to combine image analysis with the philosophy of semi-quantitative scoring systems.

The proposed methodology provides a fully automated liver biopsy image segmentation and region classification to extract CPA. The methodology is based on clustering and classification algorithms, in order to avoid manual threshold setting and image areas selection. Furthermore, it is designed to operate using low-resolution images, which can be easily obtained without any specialized equipment or time consuming manual processes, and it requires low computational effort, thus consuming very little time (image acquisition and processing needs less than a minute). Finally, the proposed methodology utilizes region characterization, in order to exclude image regions of other tissue types and artifacts from CPA extraction, thus only liver tissues contribute to the computation of the ration between fibrosis pixels and liver tissue pixels. Extensive comparative results have been extracted, combining K-means (KM) or Fuzzy C-means (FCM) algorithm for clustering stages, with several different classification algorithms for region characterization.

2. Materials and methods

The proposed methodology consists of three stages. During the first stage, clustering algorithms are used to separate background pixels from pixels belonging to all other image regions (liver tissue and all types of other tissue/artifacts). As a result, an image which includes liver tissue and all types of other tissue/artifacts on zero background is produced. In the second stage, a set of shape and color features are extracted from each region in the image. These features are used for region classification in order to identify the type of each region. Each feature vector has been annotated as liver tissue or non-liver tissue, based on experts' annotation of the corresponding image region. According to classification results, image regions classified as non-liver tissue are discarded, while regions classified as liver tissue are further processed for CPA computation. CPA is assessed is the third stage of the methodology, where clustering algorithms are applied to all pixels belonging to liver tissue regions in the image, in order to group them into two groups; the one group will include fibrosis pixels, while the other will consist of pixels of normal liver tissue. The flowchart of the proposed methodology is presented in Fig. 1.

2.1. Background/Tissue separation

The first stage of the methodology is the background/tissue separation, which is implemented using a clustering approach. To reduce dimension and time complexity stage, the image is divided into 9×9 windows, beginning from the top left pixel of the image. Then, the mean value of each window from all RGB channels is calculated, thus a feature vector with three components is calculated for each window. Then, two centroids are calculated, employing a clustering algorithm on all feature vectors of the image and setting the number of clusters equal to 2 (the first corresponding to background and the second to non-background/tissue regions).

Both KM [21] and FCM [22] clustering algorithms have been tested for the first stage.KM employs a square-error criterion, which is calculated for each of the two clusters. Iteratively, each feature vector (corresponding to a 9×9 window) of the image is assigned to the nearest centroid and then both centroid are recalculated. The iterative procedure ends when the distance between the centroids of two subsequent iterations is minimized. Similarly, FCM is based on the minimization of an objective function; however, each feature vector belongs partially in both centroids according to a membership value. After the iteratively procedure and the centroids generation, all the pixels of the images are assigned to the nearest centroid according to Euclidean distance, producing the segmented image.

With the completion of the clustering step, an image with tissue regions in zero background is produced. Then, all 8-connected regions of the image are detected and labeled, thus processing an image with labeled regions in zero background. Labeled regions with less than 500 pixels are eliminated. In Fig. 2, a liver biopsy image and the respective zero background image (produced after clustering) and the labeled image, are illustrated.

2.2. Region classification

The labeled image includes all non-background regions of the image. However, labeled regions may include several types of artifacts, which must be excluded from the CPA assessment. To address this issue, a region classification procedure has been performed. The classification procedure was designed to classify all image regions as liver tissue and non-liver tissue without differentiating the actual non-liver tissue region class (i.e. blood clot, blood vessel, muscle tissue, fat, structural collagen, dye drop, or artefact), since the main idea is to separate liver tissue regions

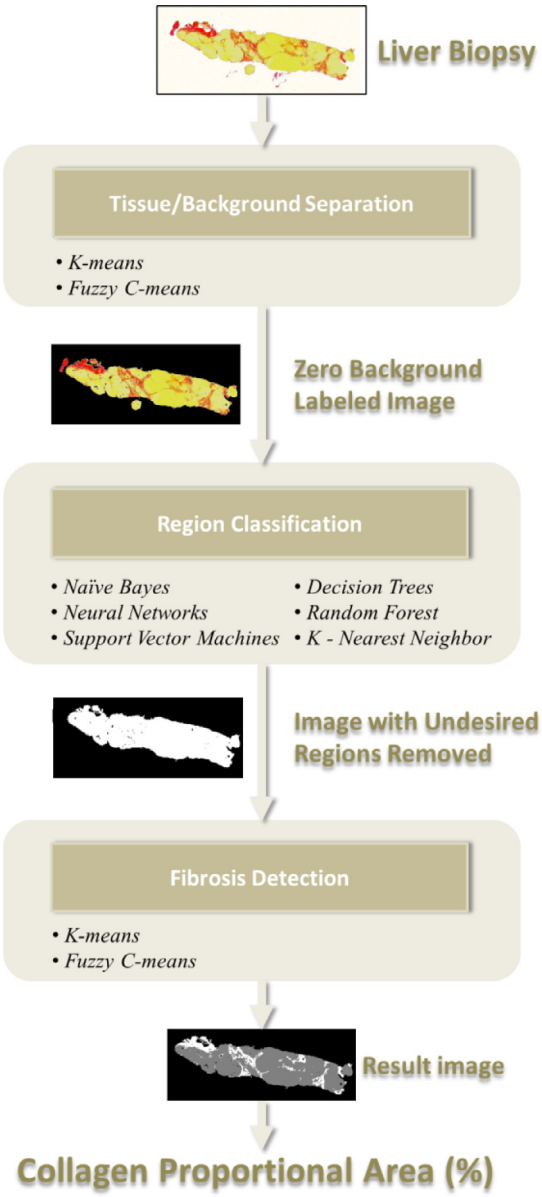

Fig. 1. Flowchart of the proposed methodology.

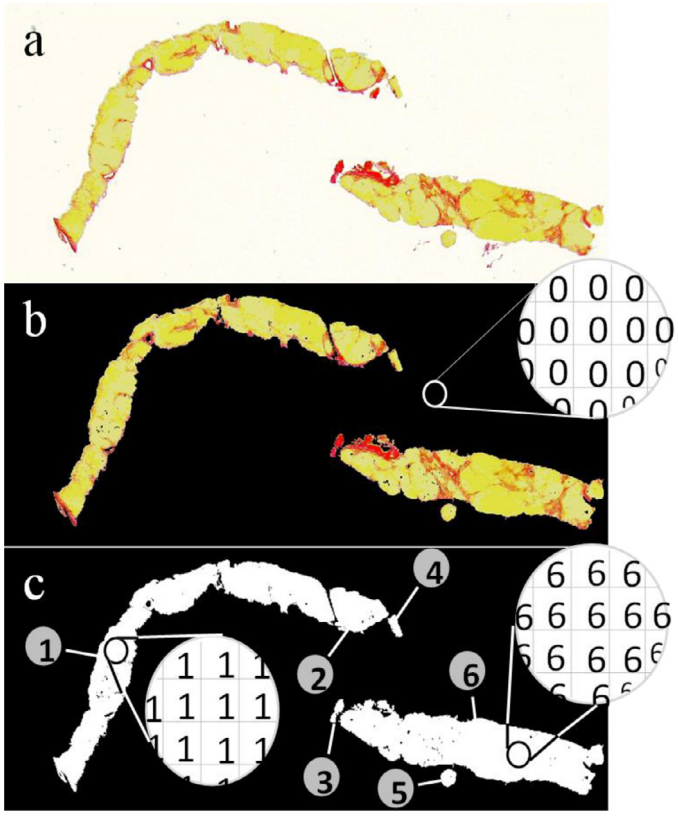

Fig. 2. Background/tissue separation stage. (a) Liver biopsy image. (b) Zero background image (c) labeled image.

Table 1
Region shape–based features.

Shape–based features	Description
Area	Number of pixels in the region
Eccentricity	Eccentricity of the ellipse that has the same second–moments as the region
Diameter	Diameter of a circle with the same area as the region
Euler number	Number of objects in the region minus the number of holes in the objects
Extent	Ratio of pixels in the region to pixels in the total bounding box
Major & minor axis length	The length (pixels) of the major & minor axis of the ellipse that has the same normalized second central moments as the region
Perimeter	Distance around the boundary of the region
Solidity	Proportion of the pixels in the convex hull that are also in the region

(which will be further processed to calculate CPA) from all other regions (which will be excluded from further process).

To classify the image regions, an informative set of features are extracted from each of them, identifying its shape and color properties. Shape-based extracted features are presented in Table 1. Color-based features are the min, max and average pixel intensity for each of the RGB channels in the image. Thus, a feature vector with 18 feature values (9 shape-based and 9 color-based) is calculated for each region. In Fig. 3, box-plots of the 18 features for liver issue and non-liver tissue regions are presented. Then, each feature vector is annotated, based on experts' characterization of the corresponding image region, as liver tissue or undesired region, with the later corresponding to blood clots, blood vessels, muscle tissue, fat, structural collagen, dye drops, and artifacts.

The annotated dataset is used to train and evaluate a classification algorithm. Six well-known classification algorithms [23–25] were tested for the second stage of the methodology in order to identify the most appropriate for this stage:

- Naïve Bayes classifier (NB).
- K Nearest Neighbor algorithm (KNN), with K = 10 nearest neighbors and the normalized Euclidean distance as distance function.
- Decision trees (DT), based on the C4.5 algorithm. The pessimistic error rate method with sub-tree replacement was employed for pruning, with at least 2 instances per leaf and 0.25 confidence factor.
- Random Forests (RF), with was created as an ensample of 10 random trees.
- Neural Network (NN), which was implemented as a Multilayer Perceptron, with 2 hidden layers, each of them having 10 neurons.
- Support Vector Machines (SVM), with a polynomial kernel.

As a result, a prediction for the type of tissue for each region of the image is generated. Regions which have been characterized as

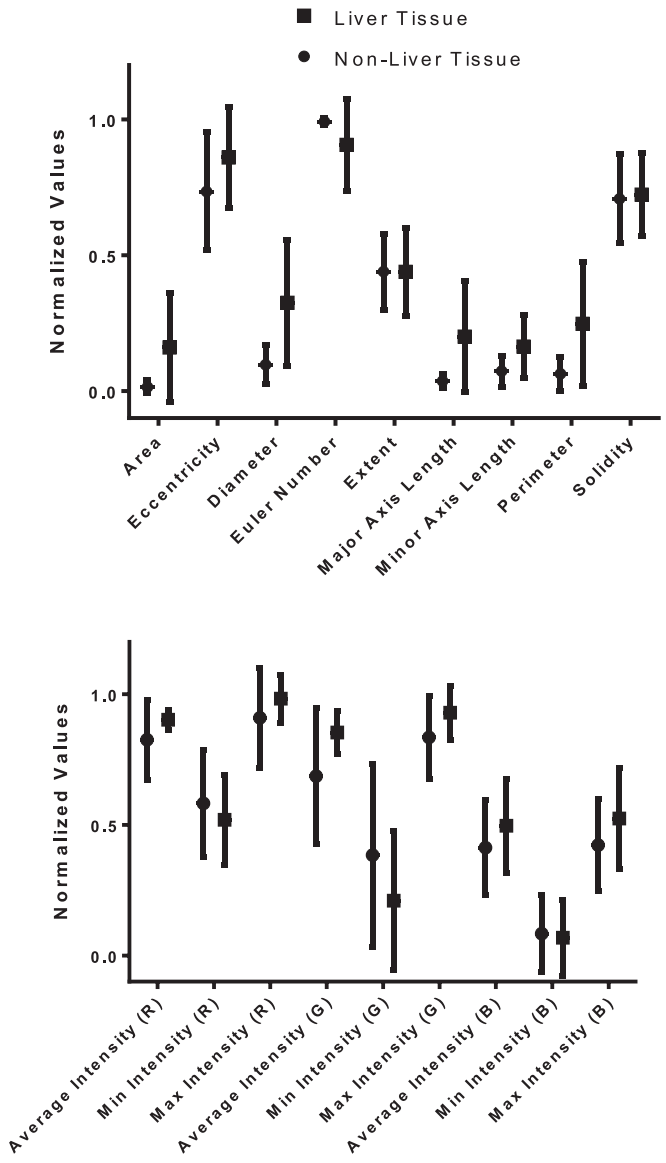

Fig. 3. Box-plots of the 18 features (using the FCM algorithm in the first stage of the methodology), shape-based (above) and color-based (below).

undesired are removed from the label image, to avoid their contribution in CPA computation. Only pixels' form regions classified as liver tissue are used as input to the third stage of methodology, to detect fibrosis expansion.

2.3. Fibrosis detection

Regions that have been classified as liver tissue are further processed in order to calculate CPA. Since pixels from background and undesired regions have been detected and removed in previous stages, fibrosis detection can be performed via a straightforward clustering (using KM or FCM). RGB values of each pixel are used for clustering, while the number of clusters is set to 2 (one for normal liver tissue pixels and the second for fibrosis). After the clustering, segmentation results from the third stage are merged with the background detection (produced in the by the first stage) extracting a resulting image: resulting image provide characterization in pixel level, similarly to the annotation of experts, where background pixels (black), normal liver tissue pixels (gray) and fibrosis pixels (white) are indicated. Fig. 4 presents the labeled image (produced by the first stage of the methodology) and the resulting image, where undesired regions (such as blood vessel and small parts of liver tissue) have been excluded by the second stage.

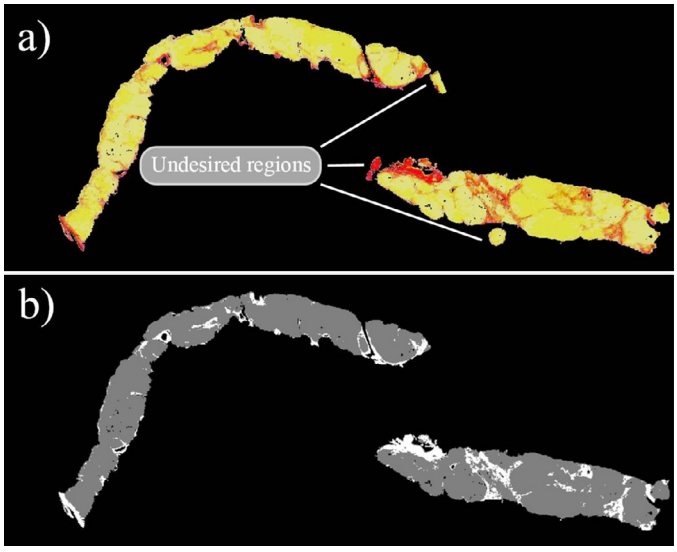

Fig. 4. Fibrosis detection stage. (a) Zero background image. (b) Resulting image (gray areas represent normal liver tissue, while white areas represent fibrosis expansions).

Collagen Proportional Area is computed as the ratio between the number of fibrosis pixels (detected in the third stage) and the number of pixels from liver tissue regions (as classified in the second stage), as follows:

$$CPA = \frac{n_{fibrosis}}{n_{fibrosis} + n_{normal\ liver\ tissue}},\ (\%) \quad (1)$$

where $n_{fibrosis}$ is the number of fibrosis pixels and $n_{normal\ liver\ tissue}$ is the number of normal liver tissue pixels.

2.4. Dataset

The proposed methodology was evaluated using a dataset of 79 images of liver biopsies, obtained from different patients with HCV. The dataset was created in the Royal Free Hospital of London. Needle liver biopsies were fixed in formalin, embedded in paraffin, and stained using Picrosirius red dye. The samples were photographed with a digital camera (Canon Powershot A640) attached to a close-up copystand with backlighting. Each sample was fitted in a single image. Low resolution images were extracted using the above equipment, in JPEG format. Specifically, the sizes of the images vary between $337 \times 1001 \times 3$ pixels and $1439 \times 1909 \times 3$ pixels. RGB color model is used, with 24 BitDepth (Filesize from 104 KB to 969 KB). Low resolution of images, gives the opportunity for fast and robust image processing. Regarding the amount of tissue presented in our set of images, there are biopsy images from two different sizes of needles. In most of the images (94.94%) one or more large tissue specimens are presented, which is sufficient according to pathologists, while in few cases (5.06%) the image contains segmented parts of tissues. Furthermore, the existence of several other types of tissue (i.e. muscular tissue, blood clot, structural collagen etc) makes the CPA measurement via image processing more challenging. All image regions, in the dataset were annotated by experts. Image regions belong to seven categories, being liver tissue, muscular tissue, blood clot, structural collagen, dye stain, artifacts and non-evaluable liver tissue (small fragments of liver tissue). The feature vector of each detected region was annotated as follows:

Table 2
CPA absolute errors (%) for all different clustering/classification algorithms.

Clustering algorithm	Classification algorithm	Total		CPA ≤ 10%		CPA > 10%	
		Mean	Std	Mean	Std	Mean	Std
KM	NB	1.79	5.36	1.35	5.06	4.04	6.49
	KNN	1.31	2.91	0.69	0.74	4.42	6.30
	DT	1.48	3.10	0.72	0.73	5.30	6.37
	RF	1.75	4.88	1.23	4.40	4.38	6.38
	NN	1.29	2.71	0.71	0.74	4.26	6.36
	SVM	1.58	3.76	1.04	2.77	4.36	5.78
FCM	NB	1.80	5.46	1.36	5.16	4.05	6.36
	KNN	1.31	3.00	0.68	0.74	4.50	6.56
	DT	1.37	2.90	0.73	0.74	4.59	6.52
	RF	1.36	2.92	0.70	0.74	4.69	6.17
	NN	1.31	2.72	0.71	0.74	4.30	6.18
	SVM	2.04	4.82	1.58	4.36	4.37	6.55

(i) if one or more detected regions were associated with a single image region, then they were annotated with the corresponding annotation,
(ii) if no detected regions were associated with an image region, then this image region was excluded from the study (no liver tissue regions fall into this case).

Since, the main concern was to remove all non-liver tissue regions from further processing (CPA calculation), the feature vectors were subsequently binary annotated as liver tissue and non-liver tissue (including all other categories). The number of patterns (i.e. annotated feature vectors from the detected image regions) is 513 (390 liver tissue and 123 non-liver tissue), when KM is employed in the first stage and 515 (392 liver tissue and 123 non-liver tissue) when FCM was employed. This difference in due to small variations in pixel segmentation (stage 1), resulting to a number of regions to be considered connected or not connected in the labeled image (after the application of the clustering algorithms). Finally, CPA for each image was assessed by experts.

3. Results

The methodology was tested using two clustering algorithms (KM, FCM) in the first and third stage and six classification algorithms (NB, KNN, DT, RF, NN, SVM) in the second stage. Each clustering algorithm was employed in both first and third stage – no combinations were tested. In the second stage of the methodology, each classification algorithm was applied to the above described dataset (i.e. features from the detected image regions) using the ten–fold stratified cross–validation procedure with respect to the number of regions. The obtained result for each region when it was placed in the test fold, was used as final classification result, and based on this classification result, the region either was rejected (if it was classified as non-liver tissue) or further processed in the third stage (if it was classified as liver tissue) in order to be used to calculate the CPA.

The final result of the methodology for each image is the CPA. All obtained CPAs using the proposed methodology were compared with the ones defined from the experts (golden standard) using Bland–Altman plots (Fig. 5), while all detailed CPA results for all different clustering/classification algorithms, for each image in the dataset are presented in the supplement.

Then, the absolute CPA error is calculated, defined as:

$$absolute\ CPA\ error\ = \left|CPA - CPA_{methodology}\right|(\%). \quad (2)$$

The absolute CPA error is calculated for all different clustering/classification algorithms, and then the mean absolute CPA error for all images, along with the absolute CPA error standard deviation, are calculated - the respective values are presented in Table 2

Table 3
Concordance correlation coefficient.

Clustering algorithm	Classification algorithm	Concordance correlation coefficient
KM	NB	0.7735
	KNN	0.9152
	DT	0.8991
	RF	0.7973
	NN	0.9229
	SVM	0.8659
FCM	NB	0.7672
	KNN	0.9116
	DT	0.9125
	RF	0.9138
	NN	0.9231
	SVM	0.7925

Furthermore, the dataset was divided in two subsets, based on the CPA value of each image (images with CPA ≤ 10% and images with CPA > 10%) and the mean value and standard deviation of the absolute CPA error for each subset was also calculated. The later was performed since according to the medical experts, small CPA values (CPA ≤ 10%) are more decisive for the patient's medical treatment than large ones (CPA > 10%).

To test the agreement between the CPA provided by experts and the CPA automatically assessed from the proposed methodology, the concordance correlation coefficient (CCC) was used [26]. CCC is a metric of the agreement between two diagnostic measurements, ranging in [− 1, 1], with value 1 corresponding to perfect agreement, value −1 to perfect disagreement, and value of 0 to no agreement. The CCC values between the actual CPA and the automatically calculated CPA, for all clustering/classification combinations, are presented in Table 3.

4. Discussion

In this work, a fully automated methodology for CPA calculation from liver biopsy images is presented. The methodology is based successive application of clustering and classification algorithms. The methodology is designed to be fully automated and to avoid any threshold-based decisions. Furthermore, all stages of the methodology are optimized with respect to the computational time.

In all different selections of clustering/classification algorithms, the total mean CPA absolute error varies from 1.29% (obtained for KM/NN) to 2.04% (FCM/SVM). In the subset of images with CPA ≤ 10%, there is a battery of clustering/classification combinations that resulted to < 0.75% in both mean CPA error and CPA error standard deviation. According to our medical experts, CPA error less than 1 is considered sufficient for patients with CPA ≤ 10%. Also, the CCC value for several clustering/classification combinations is high. When KM clustering algorithm was employed, two approaches achieved high (> 0.9) CCC values, being KM/KNN and KM/NN with 0.9152 and 0.9229, respectively, while KM/DT combination scored close to 0.9 (0.8991). In the case of FCM, 4 out of 6 combinations achieved high values, with the best being the FCM/NN with CCC value of 0.9231, which is also the overall best. The CPA and the automatically predicted CPA from the methodology using FCM clustering and NN classification, for each image of the dataset, is graphically presented in Fig. 6.

Overall, the obtained results are a strong evidence of the robustness of the proposed methodology, since they are high in the majority of the clustering/classification approaches: in 7 out of the 12 approaches CPA error is less than 0.73% (for CPA ≤ 10%) and CCC value is greater than 0.89.

The proposed methodology is designed in order to avoid threshold–based analysis, which requires human interaction and

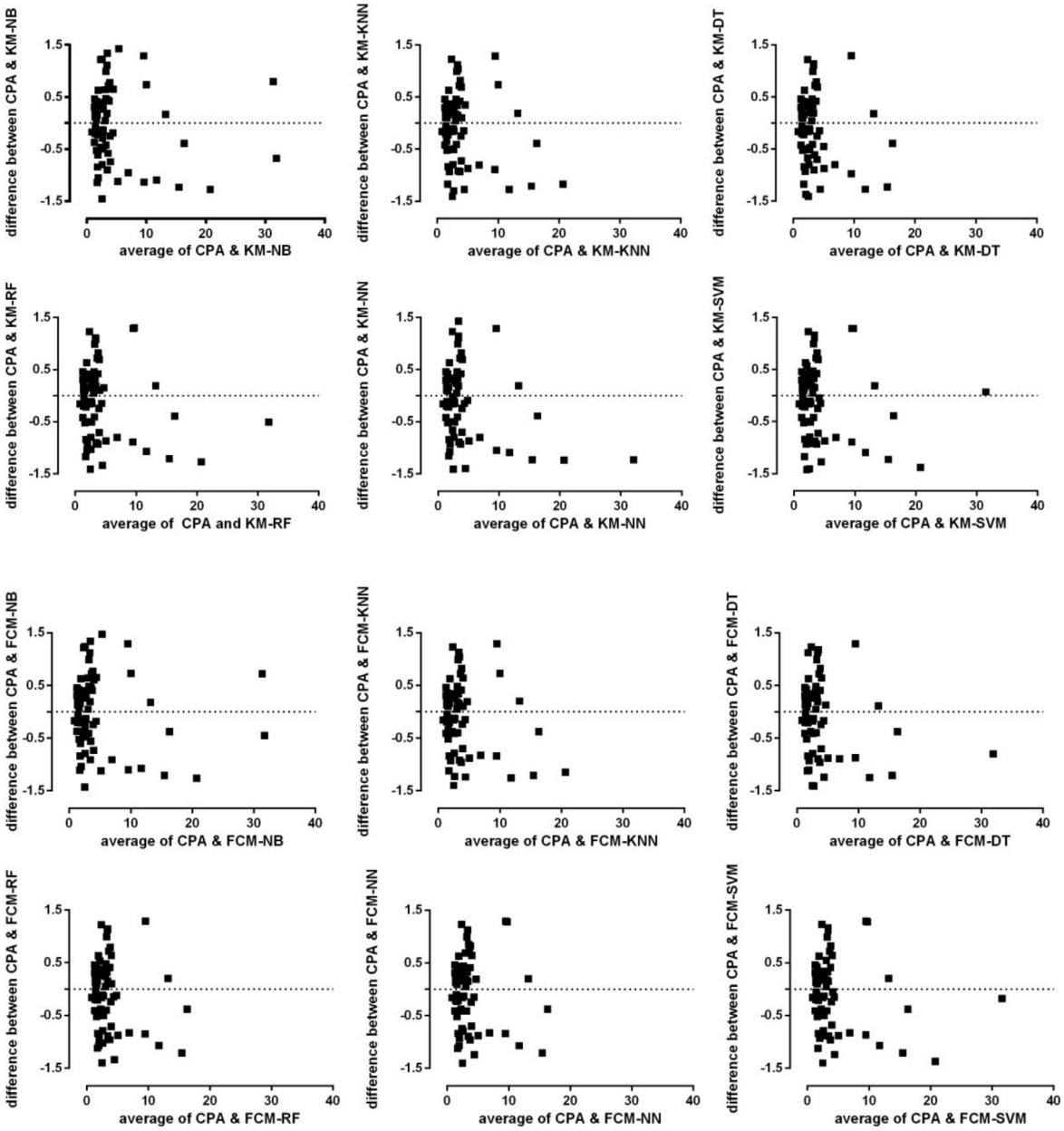

Fig. 5. Bland–Altman plots between CPAs calculated from the proposed methodology vs. CPAs defined from the experts.

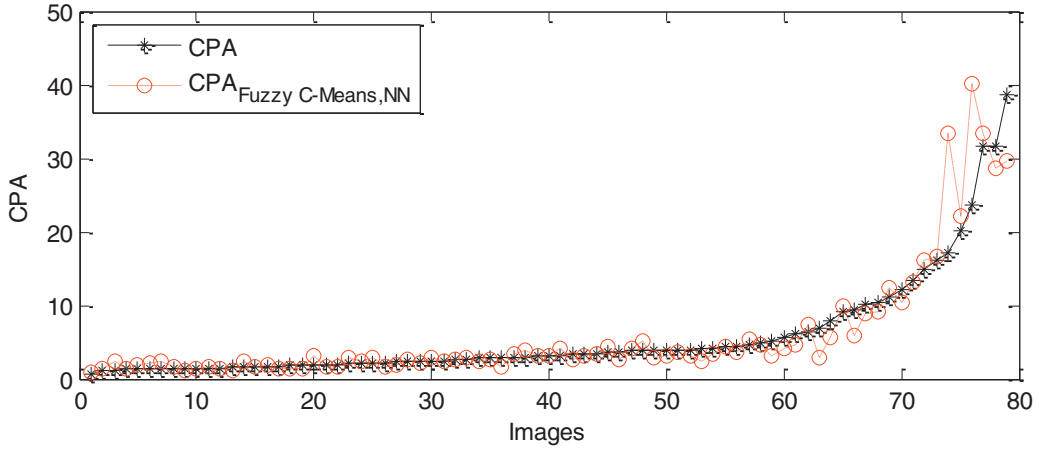

Fig. 6. CPA and calculated from the methodology CPA, using FCM and NN algorithms, for all images. The images are sorted in increasing CPA value.

manual testing. Tissue/background separation is performed using a clustering algorithm, instead of manual threshold setting widely used in the literature [2,7–12], while region classification in order to identify liver tissue regions is performed using a feature selection and classification approach, replacing manual region selection and removal commonly followed in the literature [2,7–12]. The only threshold used in the proposed methodology is the 500 pixels' limit, which follows experts' approach in image analysis, where very small regions in the image are excluded from the study, even if there are liver tissues. Thus, this step is included to speed up the second stage, since the majority of the regions eliminated from the 500 pixel threshold would also be eliminated in the second stage but through a much more computationally expensive and time consuming feature extraction/region classification procedure, and even if some were not correctly classified (and thus been further processed in the third stage), they are very small and thus have very limited impact in final CPA estimation. The elimination of threshold-based image analysis, contributes to the development of a robust methodology, free from subjective decisions, such as manual threshold trial-and-error analysis. Furthermore, clustering stages (i.e. first and third stages) produce accurate results although applied to unbalanced datasets; the liver tissue pixels / background pixels average ratio is 0.201 (stage 1) while the respective average ratio of the fibrosis pixels to the liver tissue pixels is 0.058 (stage 3).

The proposed methodology is optimized in terms of processing time, since:

(i) It is designed to process low-resolution images (all tissue from the sample is included in a single photograph).
(ii) In the tissue/background separation step (stage 1), it generates the centroids for the two clusters (liver tissue and background) using 9×9 areas, which is significantly faster than pixel-by-pixel separation. However, this only speeds up the centroid calculation procedure, since the final clustering is made pixel-by-pixel (i.e. each pixel of the image is assigned to one of the two centroids that are calculated from the 9×9 areas.
(iii) Detected regions from the first stage (which include even single-pixel regions) are filtered using a 500 pixel threshold, since they mainly correspond to noise and even if they correspond to liver tissue, they are not medically important, since highly fragmented liver tissue must be excluded from the CPA calculation. This significantly speeds up the second stage, since it drastically reduces the number of regions that will be classified.
(iv) It is fully automated. This is a major advantage of the proposed methodology compared to all other approaches presented in the literature since they either use manual threshold selection or area selection [2, 7–12], or they are based on high-resolution images, thus significantly increasing the image processing time [20]. In the second case, in the processing time it also must be added the time to acquire the image, since it is created by merging several photographs into a single image, which either requires very sophisticated equipment (i.e. a microscope with the ability to scan the sample and merge the photographs) or much more additional time (i.e. manually scan the sample and then merge the photographs).

Furthermore, the proposed methodology utilizes liver biopsy image analysis in order to automatically extract CPA, which is a medical index that has been clinically validated by numerous researches in the past two decades, while in [20] a new index is proposed (qFibrosis) which has not yet been clinically validated.

5. Conclusions

In this work a fully automated and fast operating image analysis methodology, which can be applied to easily obtained and low resolution liver biopsy images, in order to extract CPA, is presented. All the above characteristics pave the way for CPA utilization in everyday clinical practice.

The obtained results for mean absolute CPA error (Table 2) indicate that the methodology is very accurate in cases with CPA$<10\%$, with lot of the tested combinations presenting $<1\%$ absolute CPA error and standard deviation. However, the respective results in cases with CPA$>10\%$ indicate lower accuracy; the respective result for FCM/NN combination is 4.30%, with 6.18% absolute CPA error standard deviation. This is mainly associated with large fibrotic areas in the liver tissue, which are manually removed from the expert before CPA calculation. The inner-liver tissue region analysis will be addressed in future work.

Acknowledgments

This work is part funded by the by the European Union (European Regional Development Fund- ERDF) and Greek National Funds through the operational program "Thessaly-Mainland Greece and Epirus - 2007–2013" of the National Strategic Reference Framework (NSRF 2007–2013).

Supplementary materials

Supplementary material associated with this article can be found, in the online version, at doi:10.1016/j.cmpb.2016.11.012.

References

[1] F.M. Averhoff, N. Glass, D. Holtzman, Global burden of hepatitis C: considerations for healthcare providers in the United States, Clin. Infect. Dis. 55 (Jul(1)) (2012) S10–S15.
[2] V. Calvaruso, A.K. Burroughs, R. Standish, P. Manousou, F. Grillo, G. Leandro, et al., Computer-assisted image analysis of liver collagen: relationship to Ishak scoring and hepatic venous pressure gradient, Hepatology 49 (Apr) (2009) 1236–1244.
[3] R.G. Knodell, K.G. Ishak, W.C. Black, T.S. Chen, R. Craig, N. Kaplowitz, et al., Formulation and application of a numerical scoring system for assessing histological activity in asymptomatic chronic active hepatitis, Hepatology 1 (Sep-Oct) (1981) 431–435.
[4] P.J. Scheuer, Classification of chronic viral hepatitis: a need for reassessment, J Hepatol 13 (Nov) (1991) 372–374.
[5] P. Bedossa, T. Poynard, An algorithm for the grading of activity in chronic hepatitis C. The METAVIR cooperative study group, Hepatology 24 (Aug) (1996) 289–293.
[6] K. Ishak, A. Baptista, L. Bianchi, F. Callea, J. De Groote, F. Gudat, et al., Histological grading and staging of chronic hepatitis, J. Hepatol. 22 (Jun) (1995) 696–699.
[7] P. Manousou, A.P. Dhillon, G. Isgro, V. Calvaruso, T.V. Luong, E. Tsochatzis, et al., Digital image analysis of liver collagen predicts clinical outcome of recurrent hepatitis C virus 1 year after liver transplantation, Liver Transpl. 17 (Feb) (2011) 178–188.
[8] S.C. Raftopoulos, J. George, M. Bourliere, E. Rossi, W.B. de Boer, G.P. Jeffrey, et al., Comparison of noninvasive models of fibrosis in chronic hepatitis B, Hepatol. Int. 6 (Apr) (2012) 457–467.
[9] Y. Huang, W.B. de Boer, L.A. Adams, G. MacQuillan, E. Rossi, P. Rigby, et al., Image analysis of liver collagen using sirius red is more accurate and correlates better with serum fibrosis markers than trichrome, Liver Int. 33 (Sep) (2013) 1249–1256.
[10] Y. Huang, W.B. de Boer, L.A. Adams, G. MacQuillan, M.K. Bulsara, G.P. Jeffrey, Image analysis of liver biopsy samples measures fibrosis and predicts clinical outcome, J. Hepatol. 61 (Jul 2014) 22–27.
[11] H. Nakabayashi, S. Takamatsu, H. Tsujii, Y. Okamoto, H. Nakano, E. Yamada, et al., Collagen content of liver biopsy specimens in patients with chronic hepatitis, Int. Hepatol. Commun. 4 (1996) 311–315 4//.
[12] V. Calvaruso, A.P. Dhillon, E. Tsochatzis, P. Manousou, F. Grillo, G. Germani, et al., Liver collagen proportionate area predicts decompensation in patients with recurrent hepatitis C virus cirrhosis after liver transplantation, J. Gastroenterol. Hepatol. 27 (Jul) (2012) 1227–1232.
[13] C.F. Campos, D.D. Paiva, H. Perazzo, P.S. Moreira, L.F. Areco, C. Terra, et al., An inexpensive and worldwide available digital image analysis technique for histological fibrosis quantification in chronic hepatitis C, J. Viral. Hepat. 21 (Mar) (2014) 216–222.

[14] M. Kage, K. Shimamatu, E. Nakashima, M. Kojiro, O. Inoue, M. Yano, Long-term evolution of fibrosis from chronic hepatitis to cirrhosis in patients with hepatitis C: morphometric analysis of repeated biopsies, Hepatology 25 (Apr) (1997) 1028–1031.
[15] C. Pilette, M.C. Rousselet, P. Bedossa, D. Chappard, F. Oberti, H. Rifflet, et al., Histopathological evaluation of liver fibrosis: quantitative image analysis vs semi-quantitative scores. Comparison with serum markers, J. Hepatol. 28 (Mar) (1998) 439–446.
[16] M. Masseroli, T. Caballero, F. O'Valle, R.M. Del Moral, A. Perez-Milena, R.G. Del Moral, Automatic quantification of liver fibrosis: design and validation of a new image analysis method: comparison with semi-quantitative indexes of fibrosis, J. Hepatol. 32 (Mar) (2000) 453–464.
[17] T. Kurita, N. Otsu, N. Abdelmalek, Maximum likelihood thresholding based on population mixture models, Pattern Recognit. 25 (1992) 1231–1240 10//.
[18] J. Kittler, J. Illingworth, Minimum error thresholding, Pattern Recognit. 19 (1986) 41–47 /01/01 1986.
[19] T. Caballero, A. Perez-Milena, M. Masseroli, F. O'Valle, F.J. Salmeron, R.M. Del Moral, et al., Liver fibrosis assessment with semiquantitative indexes and image analysis quantification in sustained-responder and non-responder interferon-treated patients with chronic hepatitis C, J. Hepatol. 34 (May) (2001) 740–747.
[20] S. Xu, Y. Wang, D.C. Tai, S. Wang, C.L. Cheng, Q. Peng, et al., qFibrosis: a fully-quantitative innovative method incorporating histological features to facilitate accurate fibrosis scoring in animal model and chronic hepatitis B patients, J. Hepatol. 61 (Aug) (2014) 260–269.
[21] J. MacQueen, Some methods for classification and analysis of multivariate observations, in: *Proceedings of the Fifth Berkeley Symposium on Mathematical Statistics and Probability, Volume 1: Statistics*, Berkeley, Calif., 1967, pp. 281–297.
[22] J.C. Bezdek, Pattern Recognition with Fuzzy Objective Function Algorithms, Kluwer Academic Publishers, 1981.
[23] C.M. Bishop, Neural Networks for Pattern Recognition, Oxford University Press, Inc., 1995.
[24] H.B. Demuth, M.H. Beale, I. MathWorks, MATLAB Neural Network Toolbox: User's Guide, Mathworks, Incorporated, 1992.
[25] M. Kantardzic, Data Mining: Concepts, Models, Methods and Algorithms, John Wiley &; Sons, Inc., 2002.
[26] T.J. Steichen, N.J. Cox, A note on the concordance correlation coefficient, Stata J. 2 (2002) 183–189.